POAC'25
St. John's, Newfoundland and Labrador, Canada

Proceedings of the 28th International Conference on Port and Ocean Engineering under Arctic Conditions
Jul 13-17, 2025
St. John's, Newfoundland and Labrador
Canada

A novel performance representation method for icebreakers in ice using the CCGS Henry Larsen

Jungyong Wang[1], Yang Ji[2], Ayhan Akinturk[1] and Joshua Barnes[1]
[1] National Research Council, Ocean, Coastal, and River Engineering (NRC-OCRE), St. John's, Canada
[2] Marine Institute, Memorial University of Newfoundland, St. John's, Canada

ABSTRACT

This paper presents a novel approach to representing the performance of icebreakers in both model-scale and full-scale scenarios, as well as their correlation. Traditionally, icebreaker correlation studies have provided limited insights, often focusing on a few performance metrics under selected ice thickness and/or flexural strength in level ice. In some cases, pack ice conditions were used for model-scale testing, but these were rarely compared with full-scale results due to the variability in ice piece size and other environmental factors, such as waves.

Generally, icebreakers encounter a wide range of ice conditions, from loose pack ice to thick pressure ridges. However, these diverse conditions have not been comprehensively captured or analyzed in traditional ship performance assessments. To address this gap, a new method employing a non-dimensional performance curve using thrust/torque and overload coefficients was developed and applied to both model-scale and full-scale ship performance data. Additionally, the correlation between model-scale and full-scale performance was systematically evaluated and discussed.

The proposed method encompasses all potential scenarios an icebreaker may encounter, enabling the estimation of external forces, such as ice resistance, using the non-dimensional performance curve. This approach effectively transforms the ship into a sensor under various ice conditions. By utilizing performance data such as ship speed and RPM values, the method allows for the derivation of external forces, which may include a combination of ice, wave, current, and wind loads.

KEY WORDS: Icebreaker performance, model-scale/full-scale correlation

INTRODUCTION

The research focuses on advancing the performance assessment of icebreakers, particularly through the development of a novel representation method using the Canadian Coast Guard Ship (CCGS) Henry Larsen. Traditionally, the performance evaluation of icebreakers has been limited, often concentrating on a few metrics under specific ice conditions, such as selected ice thickness or flexural strength. This narrow focus has not adequately captured the diverse and challenging

environments icebreakers encounter, ranging from loose pack ice to thick pressure ridges. Such limitations highlight the necessity for a more comprehensive approach to understanding icebreaker performance across various scenarios.

The study introduces a non-dimensional performance curve employing thrust/torque and overload coefficients, which provides a holistic view of icebreaker capabilities. This method aims to bridge the gap between model-scale testing and full-scale operations, offering a systematic evaluation of performance across different ice conditions. By correlating model-scale data with full-scale measurements, the research proposes a method to transform icebreakers into sensors capable of estimating external forces, such as ice resistance. This novel approach not only enhances performance prediction but also supports ice chart validation, which is critical for navigation safety and operational efficiency.

The objectives of the study are multifaceted. First, it seeks to compare recent full-scale measurements in ice and open water with speed/power performance and associated motions. Second, it aims to develop a correlation method between model-scale results and full-scale measurements, ensuring compatibility between different testing setups. Finally, the research explores the potential of using icebreakers as sensors, leveraging performance data such as ship speed and RPM values to derive external forces, including ice, wave, current, and wind loads. This paper focuses on the first and second objectives.

Previous research, including the PAPA (Post Acceptance Performance Assessment) trial in 1988 (Stubbs et al., 1988), the ice model tests in 2020 (Wang, 2023), and the air bubbler trials in 2022 (Wang et al., 2023b), has laid the groundwork for understanding icebreaker dynamics. With continuous full-scale measurement as well as additional model tests in 2024, the study achieved significant insights into the correlation between model and full-scale performance, demonstrating the feasibility of using a non-dimensional approach to assess icebreaker capabilities comprehensively.

Through this innovative method, the research contributes to the broader field of Arctic engineering by offering a robust framework for icebreaker performance evaluation. It provides valuable insights into the dynamic interactions between icebreakers and their environment, paving the way for future studies and technological advancements. The findings have the potential to enhance operational strategies, improve ice navigation safety, and support the development of more accurate ice charting systems, ultimately contributing to the sustainable and efficient operation of icebreakers in polar regions

MODEL TEST PROGRAM OVERVIEW

Two ice tank tests and one open water test were conducted in the NRC's facility in 2020 (Wang, 2023) and 2024. In 2024 tests, all tests were performed with free-running set up, whereas the tests in 2020 was mainly towed tests in terms of resistance and powering assessment. For 2024 model tests, some ice conditions were replicated from the full-scale trial in 2022 (Wang et al., 2023b) both in ice and open water.

Ship Model and Propellers

The principal particulars of the Henry Larsen in full-scale and model-scale as well as the propeller information of the stock propeller (used for model tests) and the full-scale propeller (Larsen) are shown in Table 1.

Table 1: Principal particulars (left) and propeller information (right)

	Full-scale	Model-scale
LOA	99.8 m	4.99 m
LWL	93.8 m	4.69 m
Beam at WL	19.46 m	0.973 m
Draft	7.237 m	0.36185 m
Displacement	8225 ton	1028.125 kg
Bollard ahead thrust	678 KN	84.75 N
Wetted surface area	2230 m2	5.575 m2
AP to LCB	45.28 m	2.264 m
Block coefficient	0.61	0.61
Radius of gyration		0.35 B

	Stock	Larsen
Diameter (mm)	4120	4120
Pitch Ratio@ 0.7R	0.775	0.844
Blade Area Ratio	0.67	0.723
Hub/Prop. Diameter	0.29	0.3
10KQ at J=0	0.4	0.458
KT at J=0	0.334	0.368
# of blade	4	4
Rotation	Outward	Outward

Overload Open Water Tests

Overload open water tests were performed in the tow tank with turbulent stimulators in 2024. The measured data was further analyzed using non-dimensional coefficients, as shown in Equations 1-5. As shown in Equation 5, the thrust deduction calculation requires open water resistance. For ice breaker testing in ice, the open water portion is relatively small. Therefore, from the physical experiments in the ice tank, open water portion was measured from ice tank without turbulent stimulator and presented as a speed squared, which were acceptable for low speed with heavy ice conditions. To compare the data at speed over 12 knots, the open water portion becomes more significant, and proper prediction is necessary, which will influence the thrust deduction fraction calculation. To calculate the thrust deduction fraction from the model tests, the overload open water test results in tow tank with turbulent stimulator were used. Skin friction correction (F_D) is also considered due to the Reynolds effect from different temperature.

Figure 1 (left) shows the best fit of non-dimensional coefficients against advance coefficient (J) from the overload open water tests. These polynomials are used to calculate the ice resistance as well as ship performance prediction. Figure 1 (right) shows the thrust deduction fraction against J curve.

$$\text{Thrust coefficient, } K_T = T_{ave}/\rho n^2 D^4 \quad (1)$$

$$\text{Torque coefficient, } 10K_Q = 10Q_{ave}/\rho n^2 D^5 \quad (2)$$

$$\text{Tow force (overload) coefficient, } K_{F_X} = -Tow\ Force\ (F_X)/\rho n^2 D^4 \quad (3)$$

$$\text{Advance coefficient, } J = V/nD \quad (4)$$

$$\text{Thrust deduction fraction, } t = 1 - (-F_X + R_{OW} - F_D)/T_{sum} \quad (5)$$

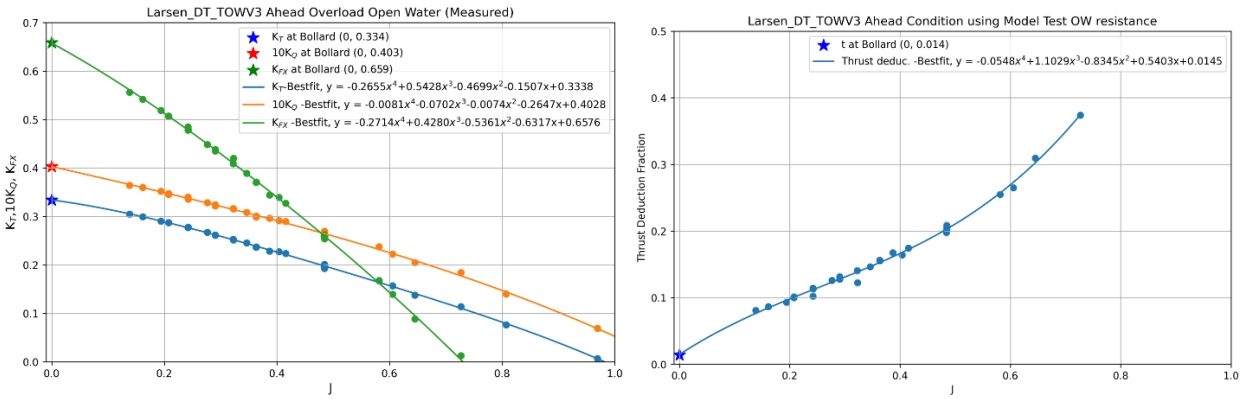

Figure 1 Overload and thrust deduction fraction with turbulent stimulator

FULL-SCALE/MODEL-SCALE COMPARISON

In this section, full-scale/model-scale comparison is made using various operating scenarios including bollard pull, level ice and various ice conditions.

Bollard Condition Comparison

RPM vs shaft power and RPM vs thrust at bollard condition were compared with full-scale measurement as shown in Figure 2. The result shows a good correlation between RPM vs thrust whereas RPM vs Power (Torque) shows well aligned until the propeller loading becomes heavy. Torque discrepancies are up to 14 % at the heaviest condition. These discrepancies may arise from slight variations in propeller geometry and complex shaft dynamics, including potential shaft vibrations and cavitation effects.

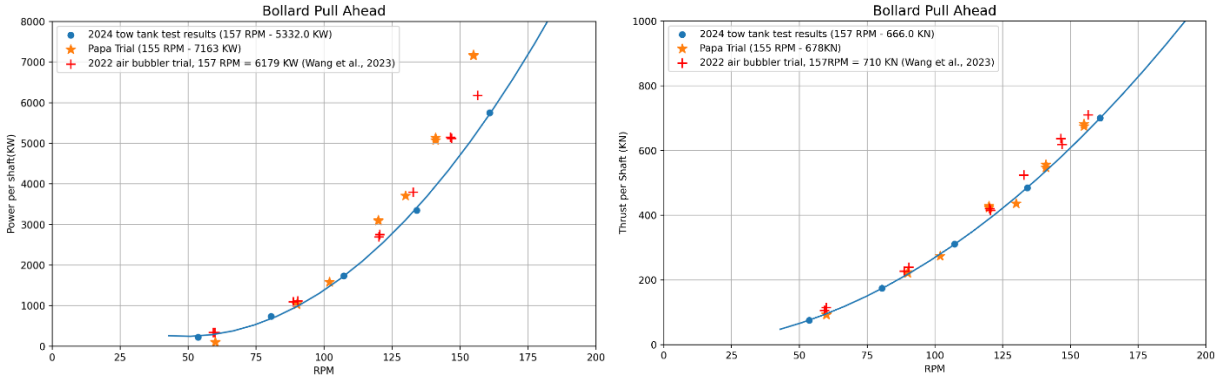

Figure 2 Bollard pull comparison

Overload Curve Correction based on the Full-Scale Bollard Pull Data

From the bollard pull tests in Figure 2, thrust values matched very well with those from full-scale measurements. However, the torque values were slightly different at higher loading conditions. To estimate the full-scale performance properly, it is necessary to adjust the torque performance curve as described above. Figure 3 shows the torque coefficient curve adjustment. Torque values were discrepant when the RPM was high (heavy loading conditions) so torque at J =0 was gradually aligned with original graph and met the same x-intercept value. It is recommended that geometrically identical propeller model should be tested and compared in the future.

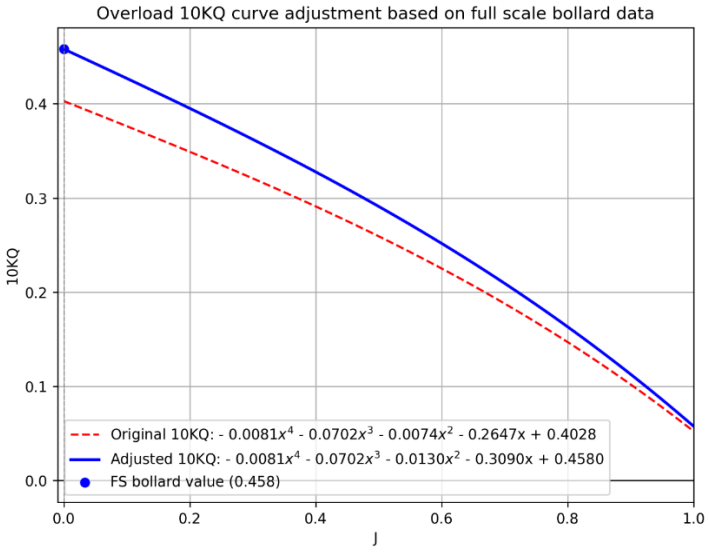

Figure 3 Overload $10K_Q$ curve correction

Ice Load Comparison

The ice load comparison section rigorously evaluates the correlation between model-scale tests conducted in an ice tank and full-scale measurements taken during air bubbler trials with the CCGS Henry Larsen. Specifically, the focus is on level ice tests performed on March 19, 2022, where key performance metrics were assessed under controlled conditions.

The comparison utilizes RPM and speed values aligned with full-scale measurements to derive power and thrust metrics from model-scale overload tests. The advance coefficient (J) was calculated from these matched values, facilitating the use of overload K_T and $10K_Q$ curves to estimate thrust and power. Ice resistance was estimated from the K_{F_X} vs J curve (see Figure 1) and the corresponding ice thicknesses (0.47 m with ice resistance of 502 kN, and 0.34 m with ice resistance of 333 kN) were derived using the ice resistance regression equation, which is shown in the following section.

Alternatively, ice resistance could also be estimated from the measured thrust values combined with thrust deduction fraction and open water resistance. The estimated values using this method were very close (495kN and 321kN) to the values calculated from the K_{F_X} values, demonstrating the validity of using K_{F_X} values

Another advantage of using the K_{F_X} vs J curve is that thrust measurement is not required to estimate the ice resistance, which provides significant benefits since thrust measurement from full-scale trials is challenging. It is noted that the full-scale ice thickness measurements varied from 0.36 to 0.55 m.

The model-scale free-running tests, despite employing higher RPMs, resulted in lower attainable speeds than full-scale measurements, potentially due to factors such as increased ice thickness and flexural strength, as well as rudder usage for course correction. This study highlights the effectiveness of the proposed non-dimensional performance curve from the overload tests in predicting ice resistance and ship performance.

Table 2 Ice load comparison between full scale and model scale

	RPM (/min)	Speed (Kts)	Thrust Sum (KN)	Power (KW)	Ice thickness (m)	Ice strength (kPa)	Est. Ice Resistance (kN)
Full scale	***144***	8.6	764	6728	0.36-0.55	530	488
Ice trial	***142***	10.3	578	5191	0.36-0.55	530	311
Model-scale	***144***	***8.6***	715	6564	0.47	530	502
Overload	***142***	***10.3***	586	5560	0.34	530	333
Model-scale	***148***	7.3	764	7418	0.48	700	609
Free running	***148***	8	718	7913	0.44	660	552

Equation 6 shows the ice resistance regression equation for the Henry Larsen model. Model tests were performed in the NRC' ice tank in 2020 and detailed test procedure and equation derivation are addressed in Wang (2023).

$$\begin{aligned} \text{Ice resistance } (R_I) \;=\; & 1.896\, S_N^{-1.66} \rho_i B h_i V_M^2 \\ & +1.448\, F_h^{-1.11} \rho_i B h_i V_M^2 \\ & +\; 1.71\, \Delta\rho g h_i B T \end{aligned} \tag{6}$$

Where, $S_N = V_M/[(\sigma_f h_i)/(\rho_i B)]^{1/2}$, $F_h = V_m/\sqrt{g h_i}$, h_i is the ice thickness, σ_f is the ice flexural strength, B is the beam of the ship at the waterline, T is the draft, ρ_i is the density of ice, $\Delta\rho$ is the density difference between ice and water, and V_m is the speed of the vessel.

Ice Resistance and Ship Performance Prediction in Various Ice Conditions

Typically, ice ship performance evaluations or correlation studies between model-scale and full-scale tests are conducted under level ice conditions(Spencer & Jones, 2001; Wang et al., 2023a; Wang & Jones, 2009). However, as discussed in the previous section, there are significant challenges associated with conducting such assessments with a limited number of data points. Variability in ice properties, even within the same ice floe, can arise from multiple factors, including environmental conditions. Relying on an average value may lead to inaccurate assessments of ship performance in ice.

Figure 4 illustrates the comparison of ice resistance between model-scale and full-scale tests across various ice conditions. For the full-scale data, data segmentation was originally conducted 100 seconds before or after the air bubbler system was activated or deactivated to assess its impact on the ship's performance, while maintaining a consistent ice condition. This segmentation approach was reused for this study but only applied when the air bubbler system was off. Because of this, the data is potentially including both transient and steady-state conditions. Note that in the legend, "T15" means "Tests on 15th of March."

Detailed ice property information, such as thickness and strength, is often unavailable for many ice conditions. However, video imagery is accessible and can be correlated with performance data in the near future. In the figures, hollow symbols with lines represent model tests in 2024, while

solid symbols indicate full-scale measurements from the 2022 bubbler trial (Wang et al., 2023b). Three distinct power levels are depicted using solid polynomials to illustrate ice loads at specific power settings.

The full-scale data contains a variety of ice and open water conditions, including level ice, thin and thick pack ice, heavy brash ice, shear zones, acceleration tests, ramming, and open water scenarios. During shear zone tests, resistance peaked as the vessel barely moved at maximum power. The vessel's operation, managed by adjusting RPM, demonstrated that multiple runs at the same tests (e.g., T17Thinfloe_Run1) did not necessarily adhere to a constant power curve; speed variations due to changing ice conditions at a constant RPM influenced power values. The graph reveals that most full-scale tests were conducted at power levels between 5191 KW and the maximum (12358 KW).

To calculate full-scale ice resistance, two methods were employed. The first method used the full-scale thrust value, combined with the thrust deduction fraction and open water resistance values. The second method utilized the K_{F_X} values from the overload open water tests. While the first method is based on full-scale thrust, the second relies solely on model tests. Comparing these two values is essential to validate their interchangeability and show good agreement as shown in Figure 5 (top). It is noted that when the ship speed exceeds 13 knots, the K_{F_X} values tend to overestimate because the hydrodynamic effect becomes more significant, making the Reynolds effect in model-scale tests dominant. From the full-scale measurement, measured power and thrust values were compared with prediction models from overload tests as shown in Figure 5 (bottom), which shows the excellent agreement.

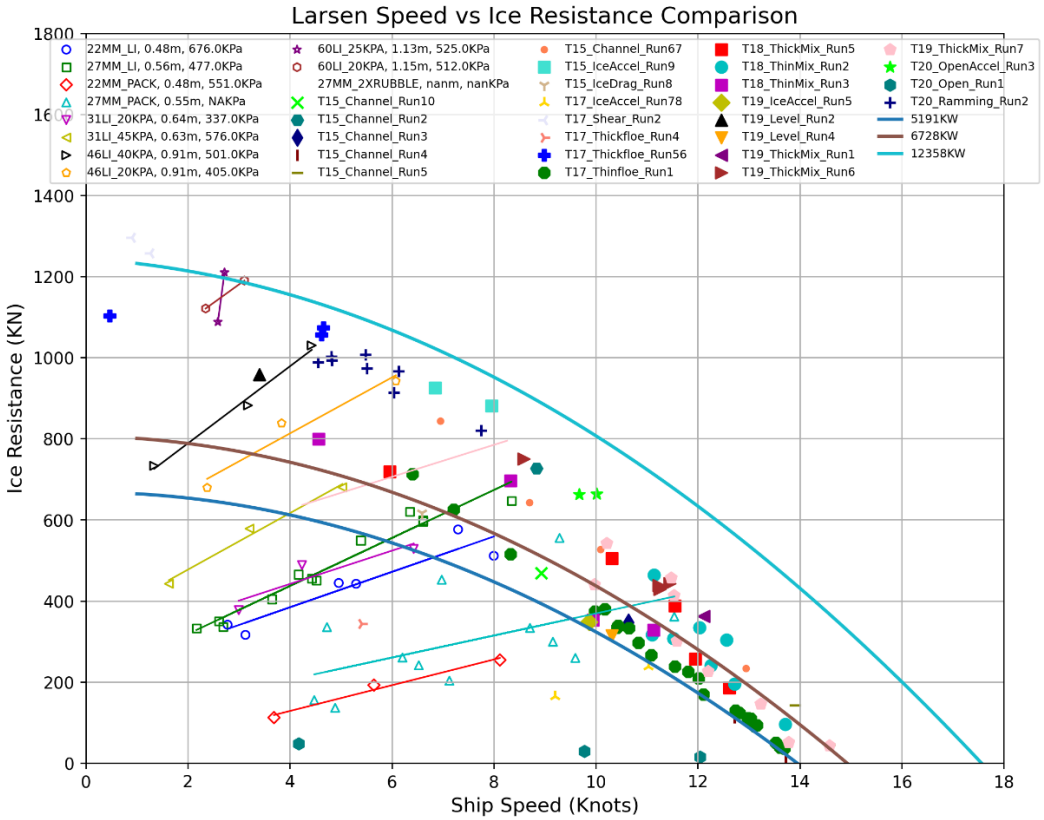

Figure 4 Ship performance graph with ship speed vs ice resistance

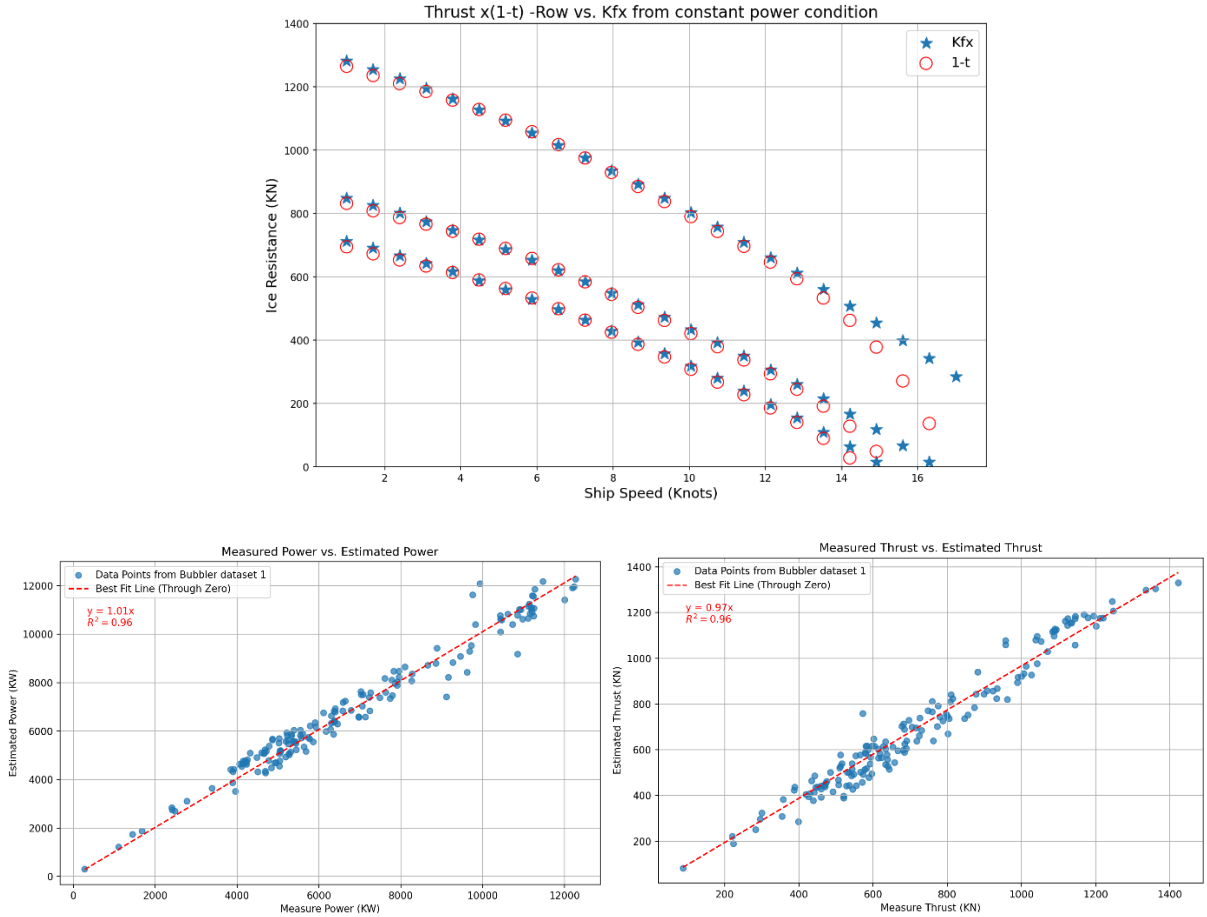

Figure 5 Ice resistance comparison (top) and measurement vs estimation for power and thrust (random 100-second dataset, bottom)

SHIP PERFORMANCE REPRESENTATION METHOD

Unlike open water condition, ice conditions can vary significantly and as shown in Figure 4, proper comparison is challenging even though uniform ice condition was tested with several ice property measurements. As described above, we prove that the ship performance (thrust and power) from the overload open water data (non-dimensional K_T, $10K_Q$, and K_{F_X}) could match quite well with full-scale measurements in ice, and this method will be an efficient tool to predict ship performance in wide range of ice conditions.

Therefore, full-scale ship performance is presented using these non-dimensional coefficients as shown in Figure 7. Main advantage is to understand the vessel performance in any overload conditions due to ice, wave, current, etc. The overload curve could act as a baseline and during ice navigation, from RPM and ship speed (or J), ice resistance can be estimated, and powering can be assessed in the real time.

In Figure 6, thrust coefficient was compared with ice tank testing (hollow symbols), full-scale measurement (solid symbols) as well as overload open water tests (solid curve). Most full-scale data are showing on or slightly above the overload curve which means generating matching or slightly higher thrust/ice resistance. Main reason could be due to the segmentations which will

likely include transient period or current/wave effect. For the model-scale data, however, they showed slightly under the curve particularly at higher J. Possible reason is to use a "booster mode" (higher RPS than the target to reduce the acceleration period with limited run length) during the tests may reduce the thrust values.

Figure 7 presents the torque coefficient comparison with a corrected torque curve using Figure 3. Both model-scale and full-scale data shows good agreement with the overload curve (solid). Generally, model-scale tests in ice generated higher torque due to larger piece sizes. For both figures, the scatter range at the same J value suggests transient dynamic effect of the propulsors. Understanding the uncertainty level in ship performance is important, and this scatter may serve as an indicator. At the same J value, lower ship speed and RPM can equate to higher ship speed and RPM to produce the same thrust and torque. Higher thrust suggests a lower inflow speed to the propeller, or vice versa, likely due to the effects of currents or waves. It is noted that the current study uses the speed over ground; however, for improved accuracy, ship speed should be measured through water.

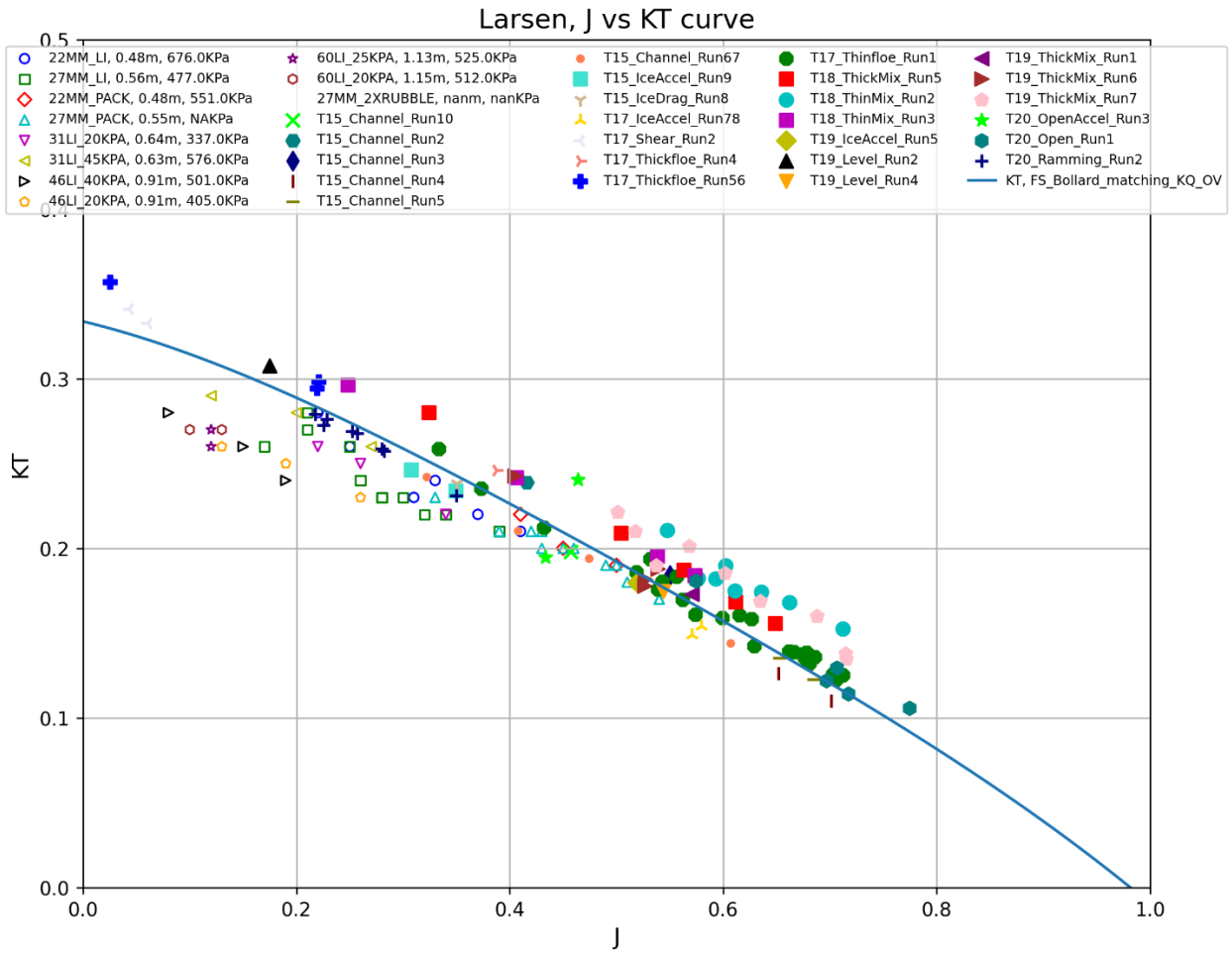

Figure 6 K_T comparison between model tests and full-scale

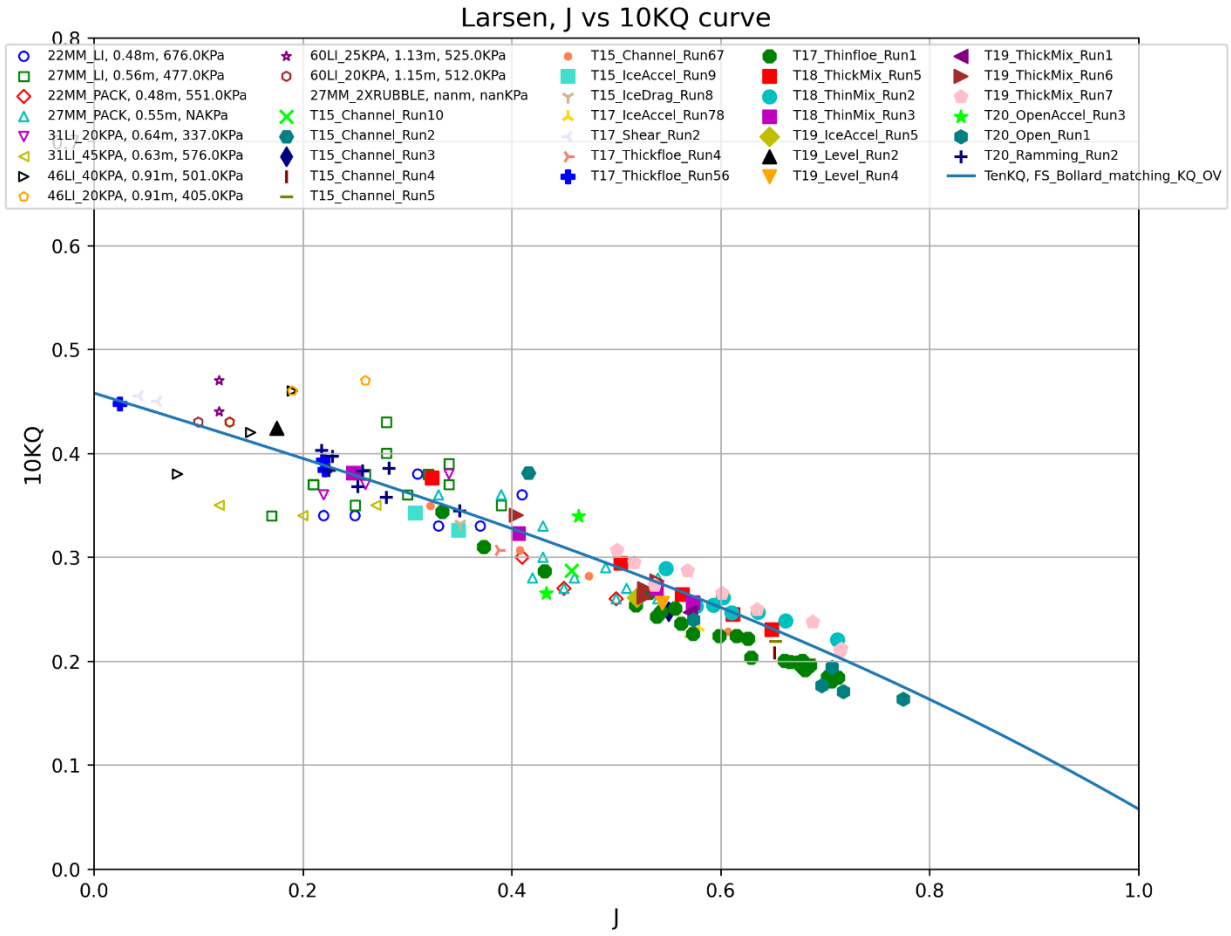

Figure 7 $10K_Q$ comparison between model tests and full-scale

Applications for Non-Dimensional Performance Curves

In addition to the representation of the ship performance in various ice conditions, this method allows the ship to function as a sensor, predicting ice conditions by equating them to an "equivalent ice thickness." For instance, an 8/10 pack ice condition with pressure can be equated to a 0.6 m thick level ice if the resistance value from the 8/10 pack ice condition is determined and the estimated ice thickness (from the ice resistance regression equation) with the same resistance is 0.6 m. This capability supports navigation systems by providing estimates of ice resistance and ship performance. Similar study was done using empirical estimation of ice resistance, open water resistance and thrust deduction fraction by Veber et al. (2023).

As more full-scale performance data and video data become available, this method will allow for the representation of various ice conditions using "equivalent level ice." Figure 8 shows the two ice field images as examples. The left and right figures can be correlated with thick blue cross and green x symbols, respectively in above performance graphs (see Figure 6 and Figure 7) Consequently, equivalent level ice resistance for those ice conditions can be predicted. Ultimately, the accumulation of such data can improve the accuracy of ice charts and support remote sensing agencies like the Canadian Ice Service. It will provide ground truth datasets as a “ship as a sensor” to validate sensing technologies, enhancing the reliability of ice navigation systems.

Figure 8 Example of ice field image (left: T17 Thickfloe_Run56, right: T15 Channel_Run10)

Additionally, this methodology is advantageous for digital twin simulations and marine training simulators by providing accurate performance outputs. It supports decision-making systems by enabling model tuning based on parameters of interest, such as emissions or expected arrival time. Within a practical range of ice and ship operating conditions, the "equivalent" level ice resistance can be pre-calculated and organized into a lookup table for quick reference, assuming sufficient correlation data between various ice conditions and equivalent level ice. Given an ice resistance value corresponding to different ice conditions, the optimal combination of ship speed and RPM can be determined, allowing for accurate ship performance simulation.

CONCLUSION

This study introduces a novel method for assessing icebreaker performance, using the CCGS Henry Larsen, across both model-scale and full-scale scenarios. By employing non-dimensional performance curves using thrust/torque and overload coefficients, the study addresses the limitations of traditional assessment methods that often focus on limited conditions and metrics. This comprehensive approach allows for an in-depth analysis of icebreaker capabilities across diverse ice conditions. A significant contribution of this research is the innovative concept of using the ship as a sensor. This enables the vessel to estimate external forces such as ice resistance in real-time, transforming it into a dynamic tool for enhancing performance prediction and supporting ice chart validation. As the ship navigates through varying ice conditions, it can provide real-time feedback on ice resistance and ship performance, which is crucial for navigation safety and operational efficiency. Furthermore, future work could involve correlating ice field image data with ship performance or ice resistance data to enhance machine learning models. By integrating visual data with performance metrics, machine learning could offer more accurate predictions of ice conditions and vessel behavior, ultimately improving navigation support systems and decision-making processes in ice-covered regions.

REFERENCE

Spencer, D., & Jones, S. J. (2001). Model-Scale Full-Scale Correlation in Open Water and Ice for Canadian Coast Guard R-Class Icebreakers. *Journal of Ship Research*, *45*(4), pp. 249–261.

Stubbs, J. T., Tam, G., Wadd, M., Koberty, R., & Witney, K. (1988). *Type 1200 PAPA trials CCGS Henry Larsen Project Report*.

Veber, J., Brown, J., Wang, J., Browne, T., Veitch, B., & Molyneux, D. (2023). A Statistical Approach for Estimating Sea Ice Thickness, in: p. V006T07A022. International Conference on Offshore Mechanics and Arctic Engineering. Retrieved from https://doi.org/10.1115/OMAE2023-101554

Wang, J. (2023). Development of an Improved Towed Propulsion Test Method in Ice to Evaluate Vessel Ice Performance Using CCGS Henry Larsen Icebreaker Model, in: p. ISOPE-I-23-283. International Ocean and Polar Engineering Conference.

Wang, J., Brown, J., & Frederking, R. (2023a). Full-Scale/Model-Scale Comparison of Podded Icebreaker's Performance in Ice with Flexural Strength Measurement Study. *Journal of Ship Research*, *67*(2), pp. 93–108.

Wang, J., Brown, J., Meadus, C., Hickey, G., Ennis, T., Winsor, F., Yulmetov, R., Baggs, J. R., & Briggs, B. (2023b). Performance Evaluation of CCGS Icebreaker Henry Larsen with Air Bubbler System in Ice, in: p. ISOPE-I-23-294. International Ocean and Polar Engineering Conference.

Wang, J., & Jones, S. J. (2009). Resistance and propulsion of CCGS Terry Fox in Ice from Model Tests to Full Scale Correlation. *Transactions - Society of Naval Architects and Marine Engineers*, *116*.